

Lightweight Design of a Machine Base for a Robot Palletizer

Ying HE^{1,2}, Jiangping MEI¹¹Tianjin University, School of Mechanical Engineering, Tianjin 300072²Ren'ai College of Tianjin University, Department of Mechanical Engineering, Tianjin 301636

Abstract — Lightweight design of a machine base of a robot palletizer is presented. The maximal stress and torque on the machine base is determined by the mechanical analysis of robot palletizer. A finite element model is established, and maximum stress, maximum deformation value and modal shape of the machine base are solved through static and modal analysis. The design variables were selected through sensitivity analysis. Using the minimal mass as the optimization objective, its approximation model was established through the Box-Behnken design and the RSM method. Also established were: i) maximum stress, ii) maximum deformation value, iii) first-order natural frequency, and iv) the scope of design variables as the constraint conditions to construct the optimization model. It was solved by using the Downhill Simplex algorithms. Our results show that on the premise of strength, stiffness and vibration stability requirement, the mass of the machine base was lightened by 8.22%.

Keywords - machine base; finite element analysis; lightweight design

I. INTRODUCTION

Stacking robot, as a method of handling and stacking, can be adaptable for the changes of handling task for its flexible action and high efficiency, which is considered as the most ideal stacking method [1] and is widely applied.

The base of stacking robot is the basic part of bearing great load, whose quality of design and manufacturing has great influence on the normal work and performance of the robot. The design criteria of base should mainly guarantee the stiffness, strength and stability of vibration. The general requirement for the design of base is to reduce weight, save material and reduce cost [2] while meeting the requirement of rigidity, strength and stiffness. Therefore, the lightweight design of base of the robot has obvious practical significance.

II. INTRODUCTION TO ROBOT AND RESEARCH PROGRAM

A. Introduction to Robot

The paper carries out research for the prototype of MD-1200YJ stacking robot. The prototype is 4 degrees of freedom articulated stacking robot, maximum load: 120kg, rotating speed of the waist: $85^\circ /s$, belonging to high speed and heavy load stacking robot [3]. It is composed of base, big arm, small arm, actuating arm of small arm, driving connecting rod of small arm, horizontal hold connecting rod, horizontal adjustment triangle arm, end effector and other parts, which is shown as Fig 1. The four driving joints from bottom to top include: waist joint above the base rotating around vertical direction, shoulder joint in big arm rotating around the direction perpendicular to the principal plane, elbow joint in small arm rotating around the same direction of shoulder joint, wrist joints in end effector rotating around the vertical direction. The feature of the mechanism is that the big arm, small arm, actuating arm of small arm, driving connecting rod of small arm, horizontal hold connecting rod,

horizontal adjustment triangle arm, end effector constitute part closed chain I, II and III, which can keep the subsurface of end effector in level pose all the time.

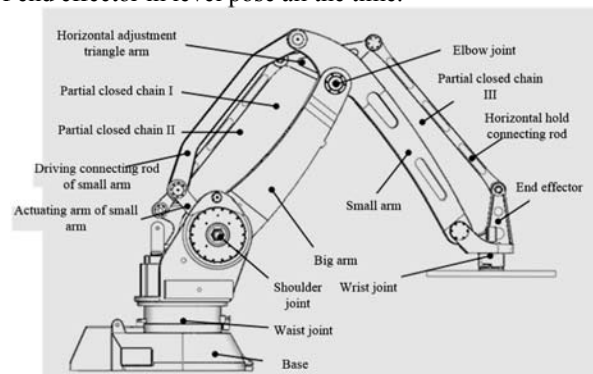


Figure 1. Structure diagram of MD-1200YJ stacking robot

B. Research Program

The research programme of the paper: analyze the stress state of working space of the robot end-effector, confirm the position of maximum stress of base. Build finite element model of base, get the maximum stress, maximum deflection (namely displacement) of initial model and modal shape through static analysis and modal analysis, providing basic data for lightweight design. Carry out optimal computation with least mass as the optimal object, with structural parameter as the design variable, with the data range of specified inherent frequency, maximum stress, maximum deflection and the design variable as constraint condition. According to the optimal results, regenerate the model using three-dimensional software and conduct comparison validation for the model before and after optimization.

III. STRESS ANALYSIS OF BASE

Take a general position of working space of stacking robot to research the stress of the base. Separate the engine

from all moving parts on it and deem all moving parts (not including load) as a whole and call it moving part by a joint name. Take the moving part as the research object. The base is connected with moving part with a RV reducer and the base is firmly connected with the ground, therefore the constraint of moving part on the engine can be deemed as constraint of fixed end. The stress analysis of moving part is shown as the Fig. 2.

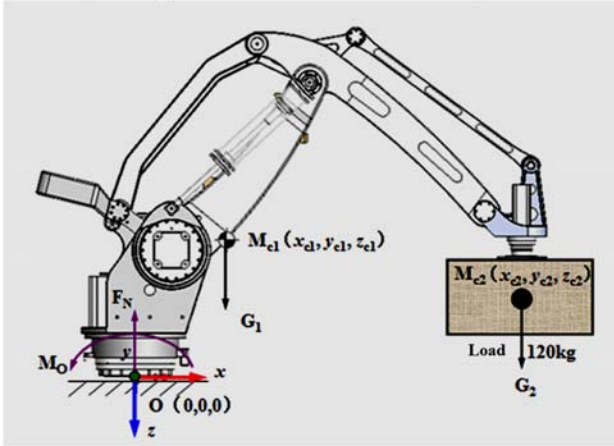


Figure 2. Stress analysis of moving part

Establish coordinate at the centre of attachment surface of waist RV reducer. O is the origin of coordinate. Z axis is vertically downward, positive direction of X axis is horizontal rightward and positive direction of y axis is perpendicular to the principal plane inwards. Supposing the Mc1 as the barycenter of moving part, its coordinate is (x_{c1}, y_{c1}, z_{c1}) and can be measured accurately by three-dimensional model, G1 is the gravity; Mc2 is the barycenter of load, whose coordinate (x_{c2}, y_{c2}, z_{c2}) can be measured accurately by three-dimensional model, G2 is the gravity. According to the equilibrium condition (1) of statics and the structure of robot, supposing the barycenter of load is on the extension cord of axis of motor rotor of end effector and taking the equilibrium formula (2)~(4) and the constraining force and moment of base on the moving part shall be solved.

$$\begin{cases} \sum F_x = 0; \sum F_y = 0; \sum F_z = 0 \\ \sum M_{ox} = 0; \sum M_{oy} = 0; \sum M_{oz} = 0 \end{cases} \quad (1)$$

$$\sum F_z = 0 \quad F_N = G_1 + G_2 \quad (2)$$

$$\sum M_{ox} = 0 \quad M_{ox} = G_1 y_{c1} \quad (3)$$

$$\sum M_{oy} = 0 \quad M_{oy} = G_1 x_{c1} + G_2 x_{c2} \quad (4)$$

According to the formula (4), we can know that the moment of attachment surface increases with the increase of distance between end and origin O, that is when the end effector of robot is in the farthest position of working space, the moment is maximum. The calculation parameter is shown as Table 1.

TABLE 1. CALCULATION PARAMETER TABLE OF BASE STRESS

Item	Parameter
G1Gravity G1	10381.61(N)
Mc1 coordinate	(554.84, -1.69, -661.92)(mm)
Gravity G2	1176(N)
xc2 coordinate of Mc2	2400(mm)

In Table 1, the x C2 value of Mc2 is the farthest distance of end effector of robot in working space. Computation result is that:

$$F_N = 11501.87 \text{ N}; \quad M_{ox} = 17.55 \text{ N}\cdot\text{m};$$

$$M_{oy} = 8582.57 \text{ N}\cdot\text{m}; \quad M_o = 8582.59 \text{ N}\cdot\text{m}.$$

Resultant moment $M_o = 8582.59 \text{ N}\cdot\text{m}$

According to Newton's Third Law, the stress and moment of attachment surface of RV reducer on base can be calculated.

IV. FINITE ELEMENT ANALYSIS OF BASE

A. Establishment of Finite Element Model of Base

The three dimensional model of base is shown as Fig. 3. And establish the finite element model on this basis.



Figure 3. Three dimensional model of base

1. Define the material property: material: QT500-7, elasticity modulus: $1.62 \times 10^{11} \text{ N/m}^2$; Poisson ratio: 0.3; shearing modulus: $6.27 \times 10^{10} \text{ N/m}^2$; density: 7000 kg/m^3 ; tensile strength: 500 MPa; yield strength: 320MPa [2].

2. Divide gridding: adopt high quality gridding, Jacobi point is 4 points; element size: 39.3301 mm; amount of node: 32071; amount of element: 17693;

3. Displacement constraint: impose full constraint on 6 mounting holes of base. The acquired finite element model is shown as Fig. 4.



Figure 4. The finite element model of base

B. Statics Analysis of Base

According to the result of stress analysis, the acquired stress and displacement cloud picture through stress analysis of base is shown as Fig. 5 and Fig. 6. The maximum value of stress is about 36.8MPa, much less than the allowable stress value of materials and the maximum of displacement is 0.0675mm. According to this, we can preliminarily ascertain that the base has the potential of lightweight design.

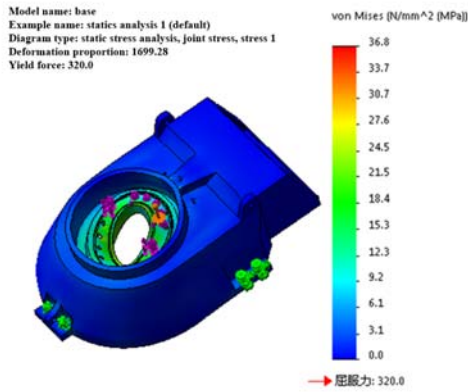


Figure 5. Cloud picture of base stress

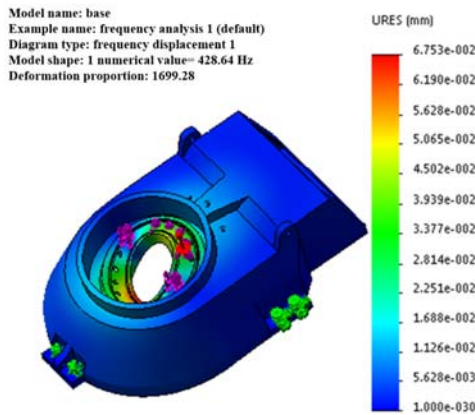


Figure 6. Cloud picture of base displacement

C. Modal Analysis of Base

The stacking robot frequently works on the complex condition of starting and stopping, reversing, grabbing and placing papers, accelerating and decelerating driving, the base is inevitable to be vibrated and impacted and as the stacking robot continuously develops to the direction of high speed, the frequency of external force effect will increase. When its value is close to the inherent frequency of base, the resonance will happen, seriously affecting the normal working of robot and even damaging the components and parts. Therefore, only statics analysis for base is not enough. The modal analysis is necessary to get inherent frequency [4], and take it into consideration as one of important factors, that means to guarantee that the structure shall have enough

high inherent frequency to avoid the resonance while conducting lightweight design.

Preprocessing of modal analysis is same as the statics analysis process, but there is no load. The paper extracts the first three modal shape Fig 7~9. Acquire the inherent frequency of the first three orders, shown as Table 2.

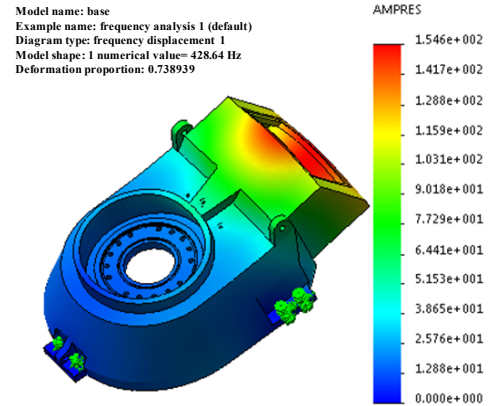


Figure 7. Vibration mode diagram of first order of base

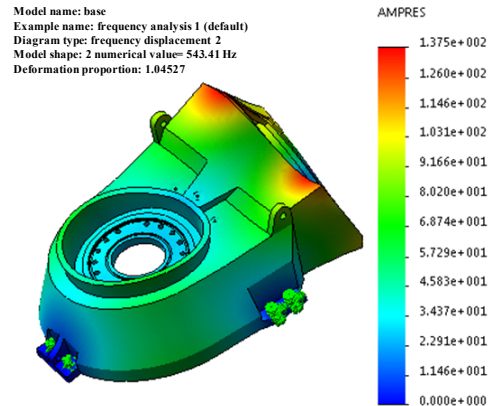


Figure 8. Vibration mode diagram of second order of base

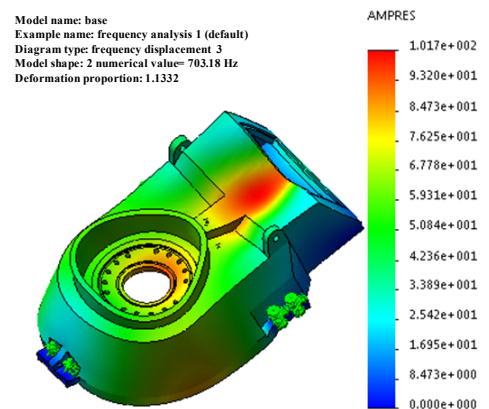


Figure 9. Vibration mode diagram of third order of base

TABLE 2. INHERENT FREQUENCY (HZ) OF FIRST FOUR ORDERS OF BASE

Number of order	1	2	3
Frequency	428.64	543.41	703.18

According to modal analysis, we can know that the inherent frequency of the first order of initial model of base is higher than the maximum frequency of exciting force of the system. Therefore, in lightweight design, we should pay attention not to reduce the inherent frequency of the first order so as to guarantee the integral rigidity of the structure and avoid the resonance phenomenon.

According to the result of finite element analysis, the primary structure of base has great potential of lightweight design.

V. LIGHTWEIGHT DESIGN OF BASE

A. Selection of Design Variable

(1) Primary selection of design variable

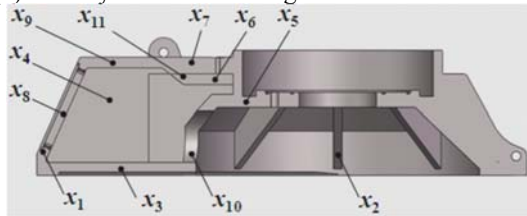


Figure 10. Selection of design variables

TABLE 3. INITIAL VALUE AND VARIATION RANGE OF DESIGN VARIABLES

Design variables	Name	Initial value (mm)	Variation range (mm)
x1	Thickness of back sloping plate	25	13~25
x2	Thickness of ribbed plate	20	8~20
x3	Thickness of base plate	25	13~25
x4	Thickness of rear side wall	25	13~25
x5	Thickness of RV attachment plate	30	13~30
x6	Thickness difference of recession of top plate	25	25~37
x7	Thickness of upper top plate	25	13~25
x8	Thickness of rear window	19	13~19
x9	Thickness of rear top plate	25	13~25
x10	Wall thickness of circular shell	30	13~30
x11	Thickness of top plate sloping plate	25	13~25

According to the structural features of base, select 11 design variables $X=(x_1,x_2,\dots,x_{11})$ shown in Fig. 10, their names, initial value and change range shown in Table 3. All design variables are just the local parameter of base. Do not change the overall dimension and the cooperative relationship with other parts and these dimension parameters are mutually independent. It will not result in the failure of modal regeneration.

(2) Sensitivity analysis of design variables

Sensitivity analysis refers to analyzing the effect degree of the changes of all design variables on the object function, selecting the structural parameter of higher sensitivity as the design variables and reducing calculated amount. The paper imposes 10% relative increment one by one for selected design variables on the basis of parameter of structural design prototype and computes the increment of performance index caused by the relative increment of design variables. Respectively acquire the mass sensitivity, inherent frequency sensitivity of the first order, stress sensitivity and deformation sensitivity and then get the comprehensive sensitivity by the sum of the four and take this as the basis of screening the design variables[6]. The comprehensive sensitivity of all design variables is shown as Fig. 11.

Select the structural parameter of over 20% comprehensive sensitivity as the optimal design variable, thus the design variable is confirmed as:

$$X=(x_1,x_2, x_3, x_5, x_8, x_9, x_{10})$$

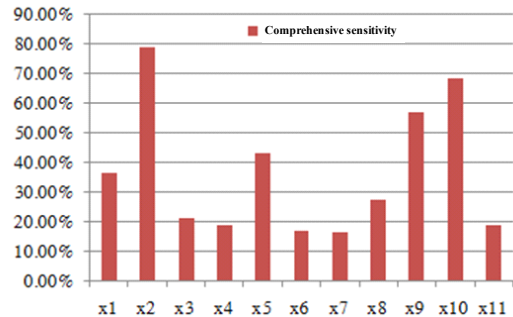


Figure 11. Comparison of comprehensive sensitivity of initially selected design variable

B. Establishment of Object Functions

Take least mass as the optimal object. According to variation range of selected design variables, the experiment design matrix table shown as Table 4 can be acquired, 57 groups in total and corresponding computing results shown as Table 5 can be got by combining Box-Behnken design method.

Take the design parameter in Table 4 as the input and the computing result in Table 4 as output, acquire the coefficient vector β of RSM[8-9] similar model of mass function is:

$$\beta=(357.4,0.45,0.45,0.49,-0.01,0.66,0.55, 0.26, 0.02,-3.6e-5,-0.0022,0.00032,0.003,0.01, -0.04,-0.004,0.003,-0.003)T$$

Select 10 groups of design parameter by adopting Box-Behnken method to be substituted into finite element model and similar model of response surface and check the computations. The result comparison is shown as Fig 12, the

error is nearly 0. It shows that the RSM model can be acted as object function to conduct optimal computation.

TABLE 4. MATRIX TABLE OF DOE EXPERIMENT DESIGN OF PART BASE

Design	Experiment number				
Variation	1	2	3	...	57
x1	19	19	19	...	19
x2	14	14	14	...	14
x3	19	19	19	...	19
x5	30	30	30	...	21.5
x8	19	19	13	...	16
x9	25	13	13	...	19
x10	21.5	21.5	21.5	...	21.5

TABLE 5. COMPUTATION RESULT OF EXPERIMENT EXAMPLE OF PART BASE

Computation	Experiment number				
Result	1	2	3	...	57
mmin(Kg)	411.59	404.54	404.54	...	407.55
f1(Hz)	427.64	438.69	438.71	...	433.23
δ(mm)	0.071	0.071	0.071	...	0.073
σ(MPa)	37.62	38.15	37.23	...	38.79

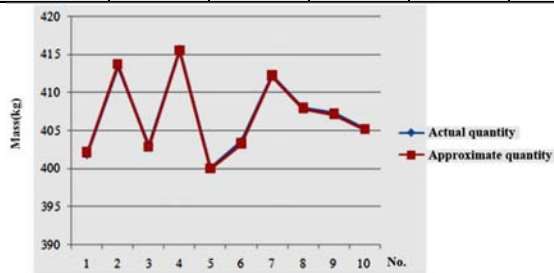


Figure 12. Precision test of RSM model

C. Constraint Function

According to design requirement, the constraint function shall include such constraints as strength, stiffness, vibration stability of structure and dimension parameter range, etc.

1.Strength constraint. The material of base is QT500-7, supposing safety coefficient $n = 2$, its allowable stress is

$[\sigma_p] = 320 / n = 160 \text{ MPa}$. Through finite element analysis, extract the maximum stress σ_{\max} , which shall meet the following conditions:

$$C_1 = \sigma_{\max} - [\sigma_p] \leq 0 \quad (5)$$

2. Stiffness constraints. Through finite element analysis, extract the maximum deformation δ_{\max} under the effect of loading. Compare it with the maximum deformation allowable value $[\delta] = 0.1\text{mm}$ required for robot design, and it shall meet the following condition:

$$C_2 = \delta_{\max} - [\delta] \leq 0 \quad (6)$$

3. Vibration stability constraint: to make the inherent frequency of structure keep away from the excitation frequency of external load. Therefore it requires that the inherent frequency of first order is not less than the inherent frequency value of same order of initial model $[f_{cn}] = 428.64\text{Hz}$ in optimization procedure, that is:

$$C_3 = [f_{cn}] - f_n \leq 0 \quad (7)$$

4. The selected design variables are the thickness dimension of plate structure, the smaller the thickness is, the lighter the mass is. Therefore, take the thickness of all plates in initial model as the maximum and select the minimum value according to the numerical value of minimum value of ductile iron casting, shown as Table 3:

D. Optimization Algorithm

The paper adopts Downhill Simplex method. This method was proposed by Nelder and Mead in 1965. Its fundamental principle is that in n-dimensional space, constitute a polyhedron with n+1 vertex, determine the goodness of fit of all vertexes and confirm the optimal point, secondary optimal point and worst point. And then find a better point through the strategy of reflection, expansion and shrinkage to replace the worst point so as to constitute new polyhedron. Repeat this process until reach the specified times or the predefined boundary value of goodness of fit and finally find or close to a optimal value point [10]. The parameter configuration of Downhill Simplex method in this paper: the accounted percentage of the initial dimension of Simplex in design space: 10%; the desirable maximum iterations is defines to: 1800.

TABLE 6. OPTIMIZATION RESULT OF STRUCTURAL PARAMETER (MM)

Structural parameter	x1	x2	x3	x5	x8	x9	x10
Before optimization	25	20	25	30	19	25	30
After optimization	13.0021944	8.004926	13.00193	22.39334	13.62551	13.00047	13.04732
Round value	13	8	13	22	14	13	13

TABLE 7. OPTIMIZATION RESULT OF PERFORMANCE PARAMETER

Object	Mass (Kg)	Inherent frequency of first order(Hz)	Maximum stress (Mpa)	Maximum deformation(mm)
Before optimization	425.75	428.64	36.8	0.06749
After optimization	390.75	435.94	39.1	0.07715
Variation	-35	7.3	2.3	0.00966

Computation Result and Analysis

Acquire structural parameter by optimization computation. The searching process is shown as Fig. 13. Conduct rounding or fine tuning for computation result by considering the factors of foundry technology parameter comprehensively, the final result is shown as Table 6. Regenerate the model according to this and acquire the optimization results of performance parameter, shown as Table 7.

The mass of base reduced by 8.22%; the inherent frequency of first order increased by about 7.3 Hz; the maximum deformation increased by about 0.00966mm; the maximum stress value increased by about 2.3Mpa, but it is still much less than the allowable stress value. The statics analysis and modal analysis of the model of after optimization is shown as Fig. 14~16. Reach the goal of reducing mass under the condition of meeting the requirement of stiffness, strength and vibration stability.

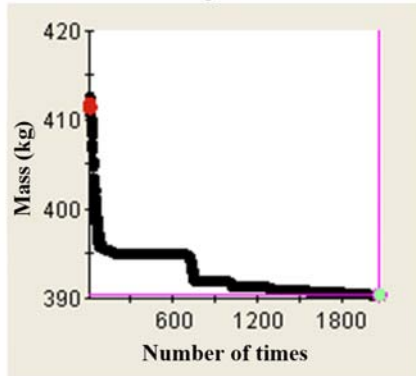


Figure 13. Searching process of least mass

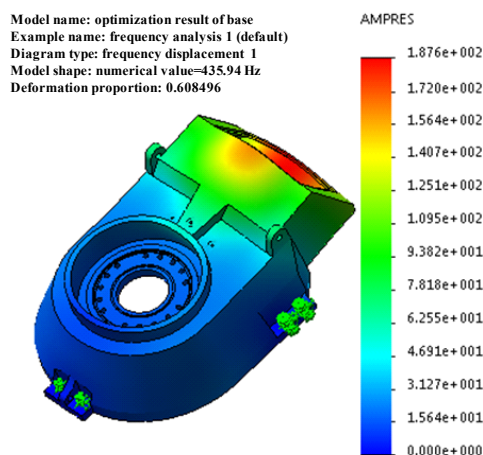


Figure 14. Vibration mode diagram of first order after optimization

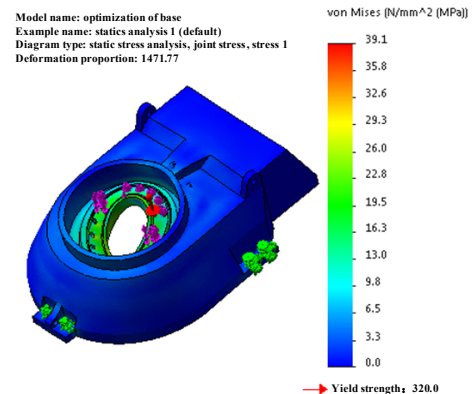


Figure 15. Stress diagram after optimization

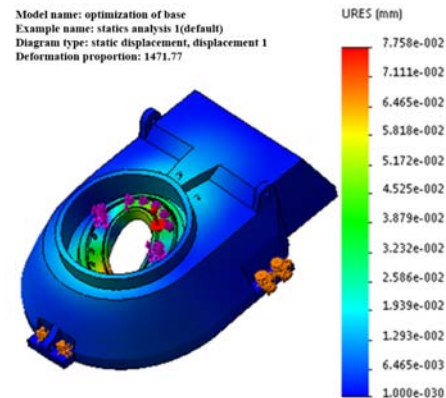


Figure 16. Displacement diagram after optimization

VI. CONCLUSIONS

This paper takes the base of model machine of MD-1200YJ stacking robot as the research object and solves the maximum value of force and moment of engine through stress analysis. Conduct statics analysis and modal analysis by finite element method. On the basis of sensitivity analysis, select the design variable and take the least mass as the optimal object and take the value range of maximum stress, maximum deformation, the inherent frequency of first order and all design variables as the constraint condition. Acquire the similar model of object functions by adopting Box-Behnken method and RSM method and conduct optimization computation by adopting Downhill Simplex method. The results show that under the condition of meeting the requirement of stiffness, strength and vibration stability, the mass reduced by 8.22%, reaching the goal of lightweight design.

ACKNOWLEDGMENTS

Project on the National Natural Science Foundation of China (51475320).

REFERENCES

- [1] Liu P, Wu Z, Wu M, et al. Study on the Kinematics Analysis and Control System at Palletizer[C]// ICLEM 2010@sLogistics For Sustained Economic Development: Infrastructure, Information, Integration. ASCE, 2015:1317-1324.
- [2] Barbash G I, Glied S A. New technology and health care costs--the case of robot-assisted surgery.[J]. *New England Journal of Medicine*, 2010, 363(8):701-4.
- [3] Ficarra V; Novara G; Artibani W; Cestari A; Galfano A; Graefen M; Guazzoni G; Guillonneau B; Menon M; Montorsi F; Patel V; Rassweiler J; Van Poppel H. Retropubic, laparoscopic, and robot-assisted radical prostatectomy: a systematic review and cumulative analysis of comparative studies.[J]. *European Urology*, 2009, 55(5):1037-63.
- [4] Fox D, Burgard W, Kruppa H, et al. A Probabilistic Approach to Collaborative Multi-Robot Localization[J]. *Autonomous Robots*, 2015, 8(3):325-344.
- [5] CANNON. Initial Experiments on the End-Point Control of a Flexible One-Link Robot[J]. *International Journal of Robotics Research*, 1984, 3(4):292-298.
- [6] Gerkey B P, Vaughan R T, Howard A. The Player/Stage Project: Tools for Multi-Robot Distributed Sensor Systems[C]// *International Conference on Advanced Robotics*. 2003:317--323.
- [7] Collins S H, Wisse M, Ruina A, et al. A 3-d Passive-Dynamic Walking Robot with Two Legs and Knees[J]. *International Journal of Robotics Research*, 2001, 20(7):607-615.
- [8] Canda A E. Re: Is Robot-assisted Radical Prostatectomy Safe in Men with High-risk Prostate Cancer? Assessment of Perioperative Outcomes, Positive Surgical Margins, and Use of Additional Cancer Treatments[J]. *European Urology*, 2015, 67(2):347.
- [9] Jinyu Hu and Zhiwei Gao. Distinction immune genes of hepatitis-induced hepatocellular carcinoma[J]. *Bioinformatics*, 2012, 28(24): 3191-3194.
- [10] Liu, Y., Yang, J., Meng, Q., Lv, Z., Song, Z., & Gao, Z. (2016). Stereoscopic image quality assessment method based on binocular combination saliency model. *Signal Processing*, 125, 237-248.
- [11] Jinyu Hu, Zhiwei Gao and Weisen Pan. Multiangle Social Network Recommendation Algorithms and Similarity Network Evaluation[J]. *Journal of Applied Mathematics*, 2013 (2013).
- [12] Yishuang Geng, Jin Chen, Ruijun Fu, Guanqun Bao, Kaveh Pahlavan, Enlighten wearable physiological monitoring systems: On-body rf characteristics based human motion classification using a support vector machine, *IEEE transactions on mobile computing*, 1(1), 1-15, Apr. 2015
- [13] Lv, Z., Halawani, A., Feng, S., Ur Réhman, S., & Li, H. (2015). Touch-less interactive augmented reality game on vision-based wearable device. *Personal and Ubiquitous Computing*, 19(3-4), 551-567.
- [14] Jinyu Hu and Zhiwei Gao. Modules identification in gene positive networks of hepatocellular carcinoma using Pearson agglomerative method and Pearson cohesion coupling modularity[J]. *Journal of Applied Mathematics*, 2012 (2012).
- [15] Jiang, D., Ying, X., Han, Y., & Lv, Z. (2016). Collaborative multi-hop routing in cognitive wireless networks. *Wireless personal communications*, 86(2), 901-923.
- [16] Borghesi M, Brunocilla E, Schiavina R, et al. Robot-Assisted Radical Nephroureterectomy for Upper Urinary Tract Urothelial Carcinoma: A Promising Alternative to Open Surgery or a Future "Gold Standard"?[J]. *Clinical Genitourinary Cancer*, 2014, 12(2):65-6.
- [17] Monn M F, Bahler C D, Flack C K, et al. The impact of hospital volume on postoperative complications following robot-assisted partial nephrectomy.[J]. *Journal of Endourology*, 2014, 28(10):1231-6.
- [18] Liu, Y., Yang, J., Meng, Q., Lv, Z., Song, Z., & Gao, Z. (2016). Stereoscopic image quality assessment method based on binocular combination saliency model. *Signal Processing*, 125, 237-248.
- [19] Yang, J., Xu, R., Lv, Z., & Song, H. (2016). Analysis of Camera Arrays Applicable to the Internet of Things. *Sensors*, 16(3), 421.
- [20] Lv, Z., Penades, V., Blasco, S., Chirivella, J., & Gagliardo, P. (2016). Evaluation of Kinect2 based balance measurement. *Neurocomputing*.